An Anti-Insulin-like Growth Factor I Receptor Antibody That Is a Potent Inhibitor of Cancer Cell Proliferation

Erin K. Maloney,[1] Jennifer L. McLaughlin,[1] Nancy E. Dagdigian, Lisa M. Garrett, Katherine M. Connors, Xiao-Mai Zhou, Walter A. Blättler, Thomas Chittenden, and Rajeeva Singh[2]

ImmunoGen, Inc., 128 Sidney Street, Cambridge, Massachusetts 02139

ABSTRACT

An antagonistic monoclonal antibody, designated EM164, has been developed which binds specifically to the human insulin-like growth factor I receptor (IGF-IR) and inhibits the proliferation and survival functions of the receptor in cancer cells. EM164 was initially selected by a rapid cell-based screen of hybridoma supernatants to identify antibodies that bind to IGF-IR but not to the homologous insulin receptor and that show maximal inhibition of IGF-I-stimulated autophosphorylation of IGF-IR. EM164 binds tightly to IGF-IR with a dissociation constant K_d of 0.1 nM, inhibits binding of IGF-I and antagonizes its effects on cells completely, and has no agonistic activity on its own. EM164 inhibits IGF-I-, IGF-II-, and serum-stimulated proliferation and survival of diverse human cancer cell lines *in vitro*, including breast, lung, colon, cervical, ovarian, pancreatic, melanoma, prostate, neuroblastoma, rhabdomyosarcoma, and osteosarcoma cancer lines. It also suppresses the autocrine or paracrine proliferation of several cancer cell lines. EM164 was the most potent antagonistic anti-IGF-IR antibody tested when compared with several commercially available antibodies. The *in vitro* inhibitory effect could be extended to *in vivo* tumor models, where EM164 caused regression of established BxPC-3 human pancreatic tumor xenografts in SCID mice. The antitumor effect of treatment with EM164 could be enhanced by combining it with the cytotoxic agent gemcitabine. These data support the development of EM164 as a candidate therapeutic agent that targets IGF-IR function in cancer cells.

INTRODUCTION

The IGF-IR[3] has been implicated in promoting oncogenic transformation, growth, and survival of cancer cells (1–4). High levels of expression of IGF-IR have been reported in a broad range of human malignancies, including synovial sarcoma, breast, prostate, colon, ovarian, and pancreatic cancer (1, 5–10). The physiological ligands of IGF-IR–IGF-I and IGF-II–are potent mitogens for diverse cancer cell lines *in vitro* (11–16). High levels of IGF-I and IGF-II expression have been noted in tumors and associated stromal cells and may stimulate cancer cell growth in an autocrine or paracrine manner (1, 17). Epidemiological studies have correlated upper quintile plasma levels of IGF-I with increased risk for prostate, colon, lung, and breast cancer (18–22). In addition to its role in proliferation of cancer cells, the IGF-IR protects cells from apoptosis caused by growth factor deprivation, anchorage independence, or cytotoxic drug treatment (2, 23, 24).

IGF-IR function has been shown to be critical for the proliferation and survival of cancer cells in a number of experimental settings. Down-regulation of IGF-IR function by antisense and dominant neg-

ative techniques reduces the growth and tumorigenicity of several cancer cell lines *in vivo* and *in vitro*, including colon cancer, melanoma, lung carcinoma, ovarian cancer, glioblastoma, neuroblastoma, and rhabdomyosarcoma (25–32). IGF-IR is thus an attractive therapeutic target based on the hypothesis that inhibition of IGF-IR function would result in selective apoptosis and growth inhibition of tumor cells (33, 34).

The IGF-IR is a transmembrane heterotetrameric protein, which has two extracellular α chains and two membrane-spanning β-chains in a disulfide-linked β-α-α-β configuration (35). The binding of its ligands (IGF-I, IGF-II) to the extracellular domains of IGF-IR activates its intracellular tyrosine kinase domain resulting in autophosphorylation of the receptor. Activated IGF-IR phosphorylates its substrates and initiates proliferative and antiapoptotic signal transduction pathways that involve phosphatidylinositol-3-kinase and mitogen-activated protein kinase (36–40). The IGF-IR is homologous to insulin receptor, sharing 84% amino acid identity in the intracellular β-chain tyrosine kinase domains and a lower 47–67% sequence identity in the extracellular α chain domains (41, 42). The high degree of homology to insulin receptor presents a considerable challenge for the development of specific small molecule inhibitors of IGF-IR tyrosine kinase activity.

A promising strategy to inhibit the function of IGF-IR in cancer cells is to apply anti-IGF-IR antibodies that bind to the extracellular domains of IGF-IR and inhibit receptor activation. Several antagonistic anti-IGF-IR monoclonal antibodies have been reported–IR3, 1H7, 24–57, 24–60, MAB391–and are commercially available. Among these previously described antibodies, the IR3 antibody has been used in several studies to inhibit the IGF-I-stimulated activation of the IGF-IR (43–46). It has also been reported that IR3 shows a weak agonistic activity when added alone to transfected murine 3T3 and CHO cell lines overexpressing human IGF-IR (47, 48). The IR3 antibody inhibits the growth of MCF-7 breast cancer cells in response to exogenously added IGF-I and IGF-II in serum-free conditions by ~80% but is only a weak inhibitor of the serum-stimulated growth of MCF-7 cells (<25% inhibition; Ref. 11). *In vivo*, treatment with the IR3 antibody did not inhibit the growth of MCF-7 tumor xenografts in athymic mice (49). In another study, a panel of antagonistic (24–57 and 24–60) and agonistic antibodies specific for human IGF-IR were obtained, which either inhibited or stimulated the binding of IGF-I to IGF-IR (50). The 1H7 antibody was reported to inhibit both IGF-I- and IGF-II-stimulated DNA synthesis in human IGF-IR-transfected 3T3 cells by ~55% (51). The commercially available IGF-IR blocking antibodies, therefore, have limitations because of their weak inhibition of the proliferation of cancer cells in response to serum or IGF-I stimulation.

The goal of the present study was to develop a potent antagonistic anti-IGF-IR antibody which significantly inhibits the serum- and IGF-I-stimulated proliferation of cancer cells and which does not show intrinsic agonistic activity. Monoclonal antibodies were raised by immunizing mice with human IGF-IR overexpressing cells or with purified full-length human IGF-IR protein. Rapid cell-based screening methods were developed for the selection of hybridoma clones based on binding to human IGF-IR-expressing cells and the absence of

binding to analogous cells expressing the human insulin receptor and for the inhibition of IGF-I-stimulated autophosphorylation of IGF-IR in MCF-7 cells.

Here, we describe an anti-IGF-IR antibody, EM164, that has potent antagonistic activity and is devoid of any measurable agonistic activity. The EM164 antibody is significantly more potent than the commercially available IR3, 1H7, and MAB391 antibodies at inhibiting the IGF-I-, IGF-II-, and serum-stimulated (or autocrine) proliferation and survival of diverse human cancer cell lines *in vitro*. Treatment with EM164, either alone or in combination with gemcitabine, inhibited the growth of BxPC-3 human pancreatic cancer xenografts in mice.

MATERIALS AND METHODS

Materials. IGF-I (recombinant human) was from York Biologicals International or Peprotech, Inc. IGF-II was from Calbiochem. Human cancer cell lines and the goat fibroblast line Ch1.Es were from American Type Culture Collection and were grown in DMEM or RPMI 1640 with 10% heat-inactivated FBS. Sera (FBS, ultra-low IgG FBS, calf serum, and adult bovine serum) were from BioWhittaker, Sigma, or Life Technologies, Inc.

The IGF-IR$^+$ and IR$^+$ cell lines that overexpress human IGF-I receptor and human insulin receptor, respectively, were obtained from Dr. Renato Baserga (52). The IGF-IR$^+$ cell line had been derived from a transfection of 3T3-like cells from an IGF-IR-deficient mouse with a human IGF-IR gene construct with Y1251F mutation in the cytoplasmic domain. The Y1251F mutation in IGF-IR does not affect the IGF-I binding and tyrosine kinase activities of the receptor. The IR$^+$ cell line overexpressing human insulin receptor had been generated in a similar manner using the same IGF-IR-deficient murine cells.

The compositions of buffers frequently used were as follows: buffer A [50 mM HEPES buffer (pH 7.4), containing 1% NP40, 2.5 mM EDTA, 100 mM sodium fluoride, 10 mM sodium PP$_I$, 10 μM leupeptin, 5 μM pepstatin, 5 mM benzamidine, 5 μg/ml aprotinin, 1 mM phenylmethylsulfonyl fluoride, 1 mM iodoacetamide]; TBS-T buffer for ELISA washes [20 mM Tris-HCl (pH 7.5), 150 mM NaCl, 0.1% Tween 20]; and ELISA blocking buffer (10 mg/ml BSA in TBS-T). In ELISA, typical incubations were at ambient temperature except for the initial coating (4°C). Experiments, including ELISA and cell cycle analysis, were in triplicate.

A biotinylated antiphosphotyrosine antibody sample was prepared by treatment of antiphosphotyrosine antibody (PY20; BD Transduction Laboratories) with NHS-LC-biotin (Pierce) at pH 8 (53). Several murine monoclonal antibodies used in this study–anti-IGF-IR-β chain-specific antibody (IgG2b) and the control antibody, B4 (IgG1)–were generated in house. The commercially available anti-IGF-IR antibodies used in this study were: IR3 (Calbiochem); 1H7 (Santa Cruz Biotechnology); and MAB391 (R&D Systems). Secondary antibodies and HRP conjugates for ELISA and Western blotting were from Jackson ImmunoResearch. MESNA and other chemical reagents were from Sigma.

Isolation of IGF-IR. Mature IGF-IR protein ($\alpha_2\beta_2$ form) was isolated from lysate of IGF-IR$^+$ cells by affinity chromatography using biotinylated IGF-I, which does not bind the unprocessed prereceptor. Biotinylated IGF-I was prepared by modification of recombinant IGF-I at 0.4–1-mg scale using any of three biotinylation reagents: sulfo-NHS-SS-biotin; NHS-PEO$_4$-biotin; or sulfo-NHS-LC-biotin (Pierce). IGF-I (0.5 mg/ml) was modified with a 5-fold molar excess of the biotinylation reagent in 0.2 M potassium phosphate buffer (pH 8) at 25°C for 2 h. The reaction mixture was quenched by addition of an amine (2-aminoethanesulfonic acid) in excess and then dialyzed in PBS at 4°C (MW cutoff 3500).

For purification of human IGF-IR, the IGF-IR$^+$ cells in 10 confluent 15-cm plates were lysed in 10 ml of buffer A on ice for 1 h. The lysate was then clarified by centrifugation, filtered over Sepharose-CL-4B beads, and finally precleared with streptavidin-agarose beads (125 μl of gel). In a separate tube, biotinylated IGF-I (100 μg) was bound to another aliquot of streptavidin-agarose beads (125 μl of gel) in buffer A at 4°C for 4 h. The beads were washed in buffer A, incubated with precleared lysate at 4°C for 10–15 h, then washed with buffer A again. The bound IGF-IR was recovered by elution with buffer A containing 4 M urea. (An alternate elution was carried out using 50

mM HEPES buffer, pH 7.6, containing 4 M urea and 0.6% w/v octyl β-glucoside.) The eluted samples were dialyzed in PBS at 4°C (MW cutoff 12,000–14,000) or were first concentrated using a Centricon Plus-20 concentrator (Millipore) before dialysis. About 100 μg of IGF-IR were recovered based on analysis by SDS-PAGE under reducing conditions using BSA protein standards and Coomassie blue staining; the purified IGF-IR sample showed α and β chain bands of M_r ~135,000 and M_r 95,000. The activity of the purified IGF-IR was confirmed by its binding to IGF-I and by tyrosine kinase assays for receptor autophosphorylation and phosphorylation of the exogenous substrate, poly(Glu-Tyr).

Generation of anti-IGF-IR Antibodies. CAF1/J and NZB/B1NJ mice were immunized i.p. with IGF-IR$^+$ cells (5 $\times$ 10^5 cells, suspended in 0.2 ml of PBS) or with purified human IGF-IR protein (30–120 μg; from urea/octyl β-glucoside elution), without or with Freund's or RIBI adjuvant. Some of the animals were boosted with 10^6–10^7 cells several times before fusion. The splenocytes from immunized mice were isolated and used to generate hybridoma with P3X63Ag8.653 cells according to standard protocols (54, 55).

The hybridoma supernatants were screened by ELISA for specific binding to the IGF-IR$^+$ cells used for immunization and for the absence of binding to IR$^+$ cells. Immulon-2HB plates (Dynatech) precoated with 100 μl of phytohemagglutinin lectin (20 μg/ml; Sigma) were charged with trypsin/EDTA-treated cells (1–3 $\times$ 10^6 cells/100 μl), centrifuged, then kept at ambient temperature for 10 min and finally dried overnight at 37°C. The wells were blocked with 5 mg/ml BSA in PBS (blocking solution) for 1 h at 37°C, washed gently with PBS, and then incubated with supernatants from hybridoma clones (diluted in blocking solution) for 1 h. The wells were washed with PBS, incubated with goat-antimouse-IgG-F$_c$$^\gamma$-antibody-HRP conjugate (0.8 μg/ml; in blocking solution) for 1 h, washed, and the binding was detected using ABTS/H$_2$O$_2$ substrate [0.5 mg/ml ABTS, 0.03% H$_2$O$_2$, 0.1 M citrate buffer (pH 4.2); 405 nm]. A hybridoma supernatant was identified, which showed strong binding to IGF-IR$^+$ cells and not to IR$^+$ cells. Using protein A affinity chromatography, a murine IgG1 κ antibody was isolated from the hybridoma supernatant and designated EM164.

Preparation of Biotinylated IGF-IR. Biotinylated IGF-IR was prepared through the reaction of intracellular cysteine residues with a biotin-PEO-maleimide reagent (53). A lysate from IGF-IR$^+$ cells was prepared using buffer A (without iodoacetamide) containing 0.3 mM MESNA (a monothiol with a low redox potential to prevent the oxidation of cysteine residues without reducing intramolecular disulfide bonds; Ref. 56). The lysate was treated with biotin-PEO-maleimide reagent (2-fold molar excess over MESNA; 4°C, 2 h). The excess biotin-PEO-maleimide was quenched by adding MESNA (equimolar to biotin-PEO-maleimide; 4°C, 2 h), and the lysate was filtered over Sepharose-CL-4B beads. The biotinylated IGF-IR from the lysate was affinity purified using anti-IGF-IR-β chain antibody (immobilized on NHS-agarose beads; Sigma), then eluted with buffer A containing 4 M urea and finally dialyzed in PBS (MW cutoff 12,000–14,000).

Binding Characterization of EM164. The dissociation constant (K_d) for the binding of EM164 to human IGF-IR was determined by ELISA methods. An Immulon-2HB plate was coated with streptavidin (10 μg/ml in 100 μl of carbonate buffer; 4°C, overnight), blocked with blocking buffer (10 mg/ml BSA in TBS-T buffer; 2 h), washed with TBS-T buffer, and then used to capture biotinylated IGF-IR (~10 ng/well) at ambient temperature for 4 h. After washing, the wells were incubated with serial concentrations of EM164 (from 5.1 $\times$ 10^{-13} to 2 $\times$ 10^{-7} M; diluted in blocking buffer) at ambient temperature for 2 h and then overnight at 4°C. After washing, wells were incubated with goat-antimouse-IgG$_{H+L}$ antibody-HRP conjugate (0.5 μg/ml) for 1 h, then washed and finally analyzed using ABTS/H$_2$O$_2$ substrate and absorbance measurements at 405 nm. The value of K_d was determined by nonlinear regression for one-site binding using the GraphPad Prism program.

For the second ELISA method, an Immulon-4HBX plate was coated directly with purified human IGF-IR (sample from urea/octyl-β-glucoside elution) in 50 mM CHES buffer, pH 9.5 (~50 ng protein; 4°C, overnight), then blocked with blocking buffer (1 h), washed, and incubated with EM164 samples or supernatants from hybridoma clones (12 h). The wells were washed and incubated with goat-antimouse-IgG-F$_c$$^\gamma$-antibody-HRP conjugate (0.8 μg/ml; 1 h), followed by washes and detection using ABTS/H$_2$O$_2$.

In a third ELISA method, a published truncated human IGF-IR α chain construct was used (57, 58). The truncated IGF-IR α chain, which lacked amino acid residues 459–690 and was fused at the COOH terminus to a

5074

(Myc)$_3$ epitope tag, was expressed by transient transfection in human 293T cells. The expressed construct was captured from the growth medium onto plates coated with rabbit anti-Myc antibody, and binding tests with EM164 were performed as described above.

To test the immunoprecipitation of IGF-IR from various cell lines by EM164, cell lysates were incubated with EM164 immobilized on protein G-agarose beads. The immunoprecipitates were analyzed by Western blot with rabbit polyclonal anti-IGF-IR β chain antibody (Santa Cruz Biotechnology; pan-specific for human, goat, monkey, hamster, and murine IGF-IR-β) and goat-antirabbit-IgG-antibody-HRP conjugate using enhanced chemiluminescence detection.

Inhibition of Binding of IGF-I to MCF-7 Cells by EM164. MCF-7 cells were incubated with $10–100$ μg/ml EM164 (or an isotype-matched control antibody) in serum-free medium (containing 1 mg/ml BSA) at 4°C or 37°C ($\sim$2 h), which was followed by incubation with 50 ng/ml biotinylated IGF-I at 4°C or 37°C (30 min). The cells were washed twice with serum-free medium and then lysed. Using a standard ELISA protocol, an Immulon-2HB plate was coated with a mouse monoclonal anti-IGF-IR-β antibody, which was used to capture the IGF-IR (and bound biotin-IGF-I) from the lysate samples. The wells were washed, incubated with streptavidin-HRP conjugate, followed by washes, and then measured using ABTS/H_2O_2 substrate.

Inhibition of IGF-IR-mediated Cell Signaling by EM164. The potential of EM164 to inhibit the IGF-I-stimulated autophosphorylation of IGF-IR and the phosphorylation of downstream effectors, IRS-1, Akt, p70 S6 kinase, and ERK, was studied in MCF-7, NCI-H838, BxPC-3, and SaOS-2 cells.

Cells were grown in 12- or 24-well plates in regular growth medium for 3 days, then washed with serum-free medium and treated with 10 μg/ml EM164 (or control antibody) in serum-free medium for $\sim$2 h. Cells were then stimulated with 50 ng/ml IGF-I at 37°C for 20 min before they were lysed in ice-cold lysis buffer containing protease and phosphatase inhibitors (buffer A, containing 2 mM sodium orthovanadate). The IGF-IR was then captured onto an ELISA plate that had been precoated with anti-IGF-IR-β antibody ($\sim$5 h). The phosphotyrosine level of the captured IGF-IR was measured by incubation with biotinylated antiphosphotyrosine antibody (0.25 μg/ml; 30 min), followed by incubation with streptavidin-HRP conjugate (0.8 μg/ml; 30 min) and detection using ABTS/H_2O_2 substrate. A similar experiment was carried out using IR$^+$ cells, which were treated with EM164 before stimulation with insulin. The insulin receptor in lysate was then captured on a plate precoated with anti-insulin receptor-β antibody (BD Transduction Laboratories), and the phosphotyrosine level was measured by ELISA.

For an indirect measurement of IRS-1 phosphorylation, an anti-IRS-1 antibody (rabbit polyclonal; Upstate Biotechnology) was captured onto an ELISA plate coated with goat-antirabbit-IgG antibody and was then used to capture IRS-1 (and bound PI3k) from the test cell lysates. The PI3k bound to phosphorylated IRS-1 was then measured by treatment with anti-p85-PI3k antibody (mouse monoclonal; Upstate Biotechnology) followed by treatment with goat-antimouse-IgG-antibody-HRP conjugate and detection using ABTS/H_2O_2 substrate.

The phosphorylation levels of other downstream effectors, Akt, p70 S6 kinase, and Erk1/2 (mitogen-activated protein kinase), were detected by Western blots of lysate samples using phosphorylation-specific antibodies (antiphospho-Akt-Ser^{473}, antiphospho-p70/p85 S6 kinase-Thr^{421}/Ser ^{424}, and antiphospho Erk1/2 rabbit polyclonal antibodies; Cell Signaling Technology), followed by incubation with goat-antirabbit-IgG$_{H+L}$-antibody-HRP conjugate and enhanced chemiluminescence detection. An anti-Akt C-20 antibody (mouse monoclonal; BD Transduction Laboratories) was used to confirm equal protein levels in all lanes.

Cell Proliferation/Survival Assays. The effect of EM164 treatment on the growth and the survival of human cancer cell lines upon stimulation by IGF-I, IGF-II, or serum was measured using the MTT assay or by cell counting after 3 days. Typically, $\sim$1500–3000 cells/well were plated in a 96-well plate in regular growth medium with serum, which was replaced with serum-free medium the next day (serum-free RPMI medium supplemented with 10 μg/ml transferrin, 1 mg/ml BSA, 50 units/ml penicillin, and 50 μg/ml streptomycin or serum-free, phenol-red-free DMEM:Ham's F-12 medium supplemented with 10 μg/ml transferrin, 2 mg/ml BSA, and 30 nM sodium selenite; Ref. 36). After 1 day of incubation in serum-free medium, the cells were washed gently with serum-free medium and then incubated with about 75 μl of 13.3 μg/ml antibody in serum-free medium for 15 min to 2 h, which was followed by the addition of 25 μl of IGF-I solution (or IGF-II solution or serum) to obtain a final concentration of 10 μg/ml antibody and 10 ng/ml IGF-I (or 20 ng/ml IGF-II or 1–10% serum). The cells were then allowed to grow for 2–3 days. A solution of MTT (25 μl of a 5 mg/ml solution in PBS) was then added, and the cells were incubated for another 2–3 h. The medium was removed and replaced by 100 μl of DMSO, and the plate absorbance was measured at 540 or 545 nm. In some experiments, IGF-I was added 15 min before the addition of EM164. Typically, four growth conditions were compared: (*a*) no IGF-I, no antibody; (*b*) no IGF-I, + antibody; (*c*) + IGF-I, no antibody; and (*d*) + IGF-I, + antibody. In some experiments, the MTT assay was replaced by counting of the cells that excluded trypan blue. As an example, MCF-7 cells ($\sim$5000 cells/well in a 12-well plate; 1 ml) were grown in DMEM with 10% FBS in the presence or absence of 5 μg/ml EM164 (or control antibody). After 5 days of growth, the cells were trypsinized and counted using a hemocytometer.

The effect of EM164 on the colony formation of HT-29 colon cancer cells was measured by plating 300 cells/well (0.4 ml of DMEM containing 10% FBS) in a 24-well plate. The cells were treated with 10 μg/ml EM164 (or control antibody) immediately after plating, and the plate was then incubated for 10 days. The colonies were stained with crystal violet.

Effect of EM164 on Apoptosis of NCI-H838 Lung Cancer Cells. The induction of apoptosis in NCI-H838 cells treated with EM164 in the presence of IGF-I (or serum) for 1 day was measured based on cleavage of cytokeratin CK18 protein (M30-apoptosense ELISA kit; Peviva).

Flow Cytometry. The specificity of binding of EM164 to IGF-IR (and not to insulin receptor) using IGF-IR$^+$ cells, and IR$^+$ cells was measured with a FACSCalibur flow cytometer. Cells were either treated with EM164, 1H7, or an anti-insulin receptor α chain antibody (BD PharMingen International) at 4°C, then with a secondary antibody-FITC conjugate at 4°C and were fixed with formaldehyde (1% in PBS) and analyzed by flow cytometry.

Cell Cycle Analysis. MCF-7 cells were serum-starved for 1 day in serum-free RPMI medium containing EM164 (20 μg/ml), washed, and treated with an additional aliquot of EM164 (20 μg/ml) for 2 h and then with IGF-I (20 ng/ml). After overnight incubation, cells were trypsinized, treated with cold 70% ethanol, propidium iodide, and RNase A, and then analyzed by flow cytometry using the LT Modfit program (Becton Dickinson).

Immunohistochemistry of Fresh-frozen Human Cancer Tissue Samples with EM164. Cryostat sections (5 μm) of fresh-frozen cancer tissue samples were fixed in acetone and stained with the Vectastain ABC Elite amplification system (Vector) as described previously (59).

Effect of EM164 as a Single Agent or in Combination with Gemcitabine in BxPC-3 Human Pancreatic Cancer Xenograft in Mice. Human pancreatic cancer xenografts were established in 5-week-old, female SCID/ICR mice (Taconic) by s.c. injections of 10^7 BxPC-3 cells in PBS (day 0). When the tumors had reached a volume of $\sim$80 mm^3 (day 11), the mice were randomized by tumor volume into five groups of five animals each. The five groups were treated with EM164 alone (13 injections of 0.8 mg/mouse, i.v., lateral tail vein, on days 12, 16, 19, 23, 26, 29, 36, 43, 50, 54, 58, 61, and 64), with gemcitabine alone (two injections of 150 mg/kg/mouse, i.p., on days 12 and 19), with a combination of gemcitabine and EM164 following the above schedules, PBS alone, and a control antibody alone (using the same schedule as EM164). The tumor sizes were measured twice each week using the LABCAT system.

RESULTS

Identification of an Inhibitory anti-IGF-IR Monoclonal Antibody through a Rapid Biological Screen. To generate monoclonal antibodies, CAF1/J and NZB/B1NJ mice were immunized and subsequently boosted either with murine IGF-IR$^+$ cells that express high numbers of human IGF-IR ($\sim$10^7/cell) or with purified human IGF-IR protein. The generated hybridoma supernatants were screened by cell-based ELISA methods for specificity of binding and biological activity. Supernatants were selected that contained IgG antibodies that bound to the IGF-IR$^+$ cells used for the immunization and not to the analogous IR$^+$ cells that express human insulin receptor. In a second screen, the antibody with the desired binding specificity was purified and then assayed for its inhibitory activity in an IGF-I-stimulated IGF-IR autophosphorylation assay using MCF-7 breast cancer cells.

5075

From eight fusions, 1216 hybridoma supernatants were screened for binding, yielding 61 clones, which bound selectively to IGF-IR$^+$ and not to IR$^+$ cells. These selected clones were further subcloned and then tested again for specific binding and for inhibition of IGF-I-stimulated IGF-IR autophosphorylation. A potent inhibitory antibody, EM164 (mouse monoclonal IgG1 κ), secreted by a hybridoma generated from a CAF1/J mouse immunized with IGF-IR$^+$ cells, was selected for additional studies.

A flow cytometry experiment confirmed that EM164 bound selectively to murine IGF-IR$^+$ cells expressing the human IGF-IR and not to the equivalent IR$^+$ cells expressing the human insulin receptor (Fig. 1A). A dissociation constant (K_d) of 0.1 nM was measured for the binding of EM164 to biotinylated IGF-IR with an ELISA in which the biotinylated IGF-IR had been captured with a streptavidin-coated plate (Fig. 1B). To ensure that the extracellular α chain of IGF-IR was not altered by biotinylation, a biotinylation method was used which only modifies cysteine residues (and not cystine residues) because cysteine residues are only present intracellularly in the β chain. An identical K_d (0.1 nM) was measured with an ELISA in which purified unmodified IGF-IR was coated directly onto an ELISA plate. The Fab fragment of EM164 (prepared by papain digestion) showed a similar K_d value of 0.3 nM in the biotinylated IGF-IR binding ELISA, indicating that the high affinity binding observed with the bivalent EM164 antibody represented predominantly monomeric binding. The purities of the IGF-IR and EM164 samples used in the binding studies and all other studies were confirmed by SDS-PAGE using Coomassie blue staining (Fig. 1C).

To test the effect of EM164 on the activity of IGF-IR and insulin receptor, MCF-7 cells and IR$^+$ cells were stimulated with IGF-I or insulin, respectively, in the presence or absence of EM164. The phosphotyrosine levels of activated IGF-IR and activated insulin receptor were then measured by ELISA. EM164 showed potent inhibition of the IGF-I-stimulated autophosphorylation of IGF-IR in MCF-7 cells (Fig. 2A). In contrast, EM164 had no effect on insulin-stimulated autophosphorylation of insulin receptor in IR$^+$ cells, thus additionally confirming the specific inhibition of IGF-IR by EM164 (Fig. 2B).

EM164 Binds to the IGF-IR in Human Cancer Tissue Samples. The binding of EM164 to IGF-IR in human cancer tissue samples (breast, colon, and lung) and in several cell lines (human, monkey, goat, hamster, rat, and mouse) was tested by immunohistochemistry and by immunoprecipitation. Immunohistochemical analyses of fresh-frozen human cancer tissue samples with EM164 showed a moderate to strong staining for two of three breast cancer samples, one of one lung cancer sample, and a weak to moderate staining for three of three colon cancer samples. EM164 also showed moderate to strong staining in the corresponding normal tissues of breast (ducts and lobules), lung (bronchial epithelium), and colon (smooth muscle and epithelial mucosa). The staining of the infiltrating ductal carcinoma cells of a breast cancer sample and of the ductal epithelial cells of a normal breast tissue sample by EM164 is shown in Fig. 2C.

The specificity of the binding of EM164 to IGF-IR from different species was determined by an immunoprecipitation experiment using lysates from various cell lines, which showed that EM164 bound to IGF-IR from human (MCF-7 and 293) and African green monkey (COS-7) cells. EM164 did not immunoprecipitate IGF-IR from mouse (3T3), rat (Rat 1), Chinese hamster (CHO), and goat (goat fibroblast) cells (data not shown). In a human cell lysate sample prepared with SDS under denaturing conditions, the IGF-IR was not detected using EM164 in a Western blot, thus indicating that the binding of the antibody is dependent on the native conformation of the IGF-IR (data not shown). EM164 bound with high affinity to a truncated human IGF-IR α chain lacking
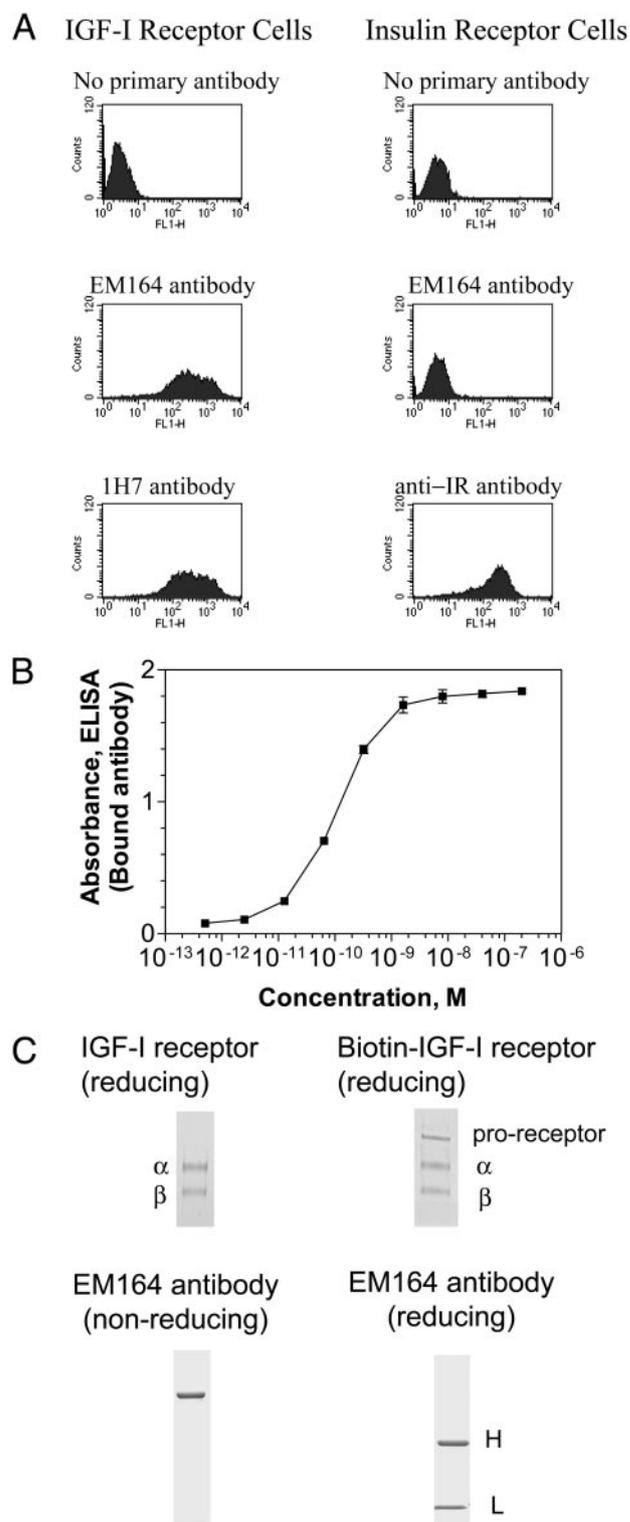

Fig. 1. Binding of EM164 to IGF-IR but not to insulin receptor. *A*, flow cytometry of human IGF-IR-expressing cells and human insulin receptor-expressing cells treated with 100 nM EM164 antibody, no primary antibody, or positive control antibodies (1H7 antibody for IGF-IR cells and anti-insulin receptor antibody for insulin receptor cells). *B*, ELISA binding titration curve for binding of EM164, at various concentrations, to biotinylated IGF-IR captured on coated streptavidin. *C*, SDS-PAGE (Coomassie blue staining) of purified IGF-IR, biotinylated IGF-IR, and EM164 under reducing and nonreducing conditions.

amino acid residues 459–690, which shows that the epitope recognized by the antibody is in the NH$_2$-terminal portion (amino acids 1–458) and/or in the 16 amino acids (691–706) of the COOH terminus of the extracellular α chain (data not shown).
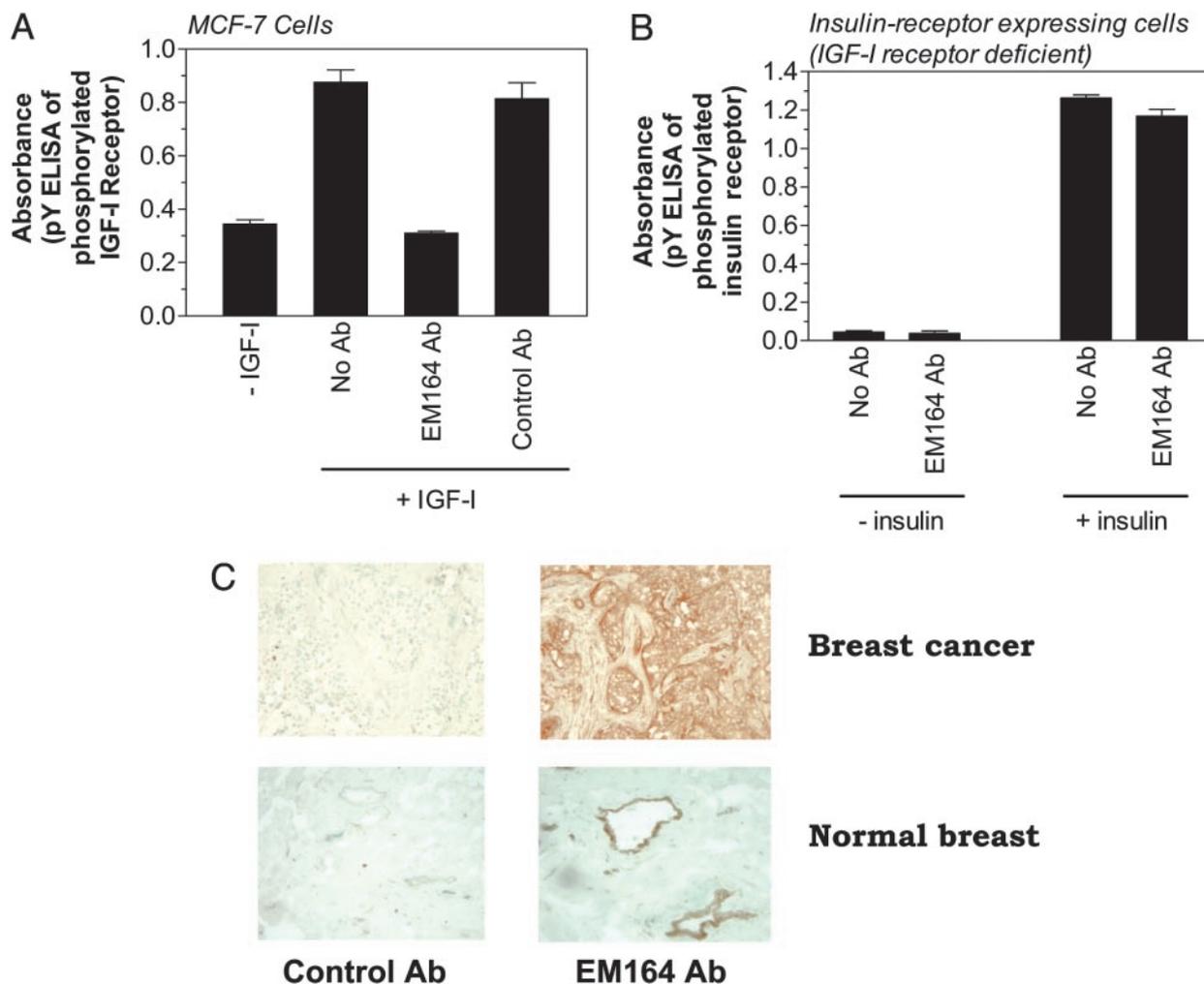
Fig. 2. Specific inhibition of IGF-IR in human cancer cells by EM164 and immunohistochemistry of human cancer tissue using EM164. *A*, inhibition of IGF-I-stimulated autophosphorylation of IGF-IR in MCF-7 cells by EM164. MCF-7 cells were incubated with EM164 or control antibody (10 μg/ml) for ~2 h and then stimulated with IGF-I (50 ng/ml) for 20 min. The cell lysates were analyzed by ELISA, based on the capture of IGF-IR using coated anti-IGF-IR β chain antibody, followed by measurement of phosphorylation level of captured IGF-IR using biotinylated antiphosphotyrosine antibody and streptavidin-HRP conjugate. *B*, EM164 did not inhibit insulin-stimulated autophosphorylation of insulin receptor in a similar experiment with insulin-receptor expressing cells. *C*, immunohistochemistry of infiltrating ductal carcinoma of breast and normal breast tissue using EM164 and a control antibody.

EM164 Inhibits the Binding of IGF-I to IGF-IR. To determine whether EM164 inhibited the binding of IGF-I to IGF-IR, competition binding experiments were performed using EM164, biotinylated IGF-I, and MCF-7 cells at the physiological temperature of 37°C and also at 4°C to minimize the down-regulation of the IGF-IR. Cells were first incubated with EM164 (10–100 μg/ml; 60–600 nM) for 2 h and then with biotinylated IGF-I (50 ng/ml; 6 nM) for 30 min. The cells were then cooled on ice, lysed, and the IGF-IR in the lysate samples were captured onto an ELISA plate coated with an anti-IGF-IR β chain antibody. The receptor-bound biotinylated IGF-I was then measured by ELISA. Treatment with saturating concentrations of EM164 resulted in a strong inhibition (~90% inhibition) of the binding of IGF-I to IGF-IR in cells at both 4°C and 37°C (Fig. 3, *A* and *B*).

To evaluate the potential down-regulation of IGF-IR by EM164 treatment at 37°C and 4°C, the level of IGF-IR β chain in EM164-treated MCF-7 and BxPC-3 cells was assessed by Western blotting with a polyclonal anti-IGF-IR-β antibody. At 37°C, no decrease in the amount of IGF-IR β chain in the Western blot was seen during the first 30 min of treatment with EM164, but a slight decrease was apparent upon a longer incubation of 1–2 h and was accompanied by the appearance of bands for degraded β chain (Fig. 3, *C* and *D*). For EM164-treated cells at 37°C, about a 25% down-regulation of the receptor was observed after 2 h, which increased to ~50% after 4–8 h and to 50–75% after 24 h, based on a comparison with diluted fractions of the untreated control sample (Fig. 3*D*; data not shown). This down-regulation of IGF-IR-β by EM164 at 37°C was similar to that observed in this study with other anti-IGF-IR antibodies IR3, 1H7, and MAB391 (data not shown). In contrast, no down-regulation of IGF-IR-β was observed upon treatment with the ligand, IGF-I, at 37°C for 24 h. As expected, no down-regulation of IGF-IR-β was observed upon treatment with EM164 for 2 h at the lower temperature of 4°C (Fig. 3*C*).

EM164 Inhibits IGF-IR Signaling in Cells. The effect of EM164 on the IGF-I-stimulated activation of IGF-IR and the downstream signaling was measured in MCF-7 breast cancer, NCI-H838 lung cancer, BxPC-3 pancreatic cancer, and SaOS-2 osteosarcoma cell lines. Cells were treated with EM164 for 30 min to 2 h and then stimulated with IGF-I for 20 min. The cells were then lysed and the lysates were analyzed for the phosphorylation levels of effector proteins in the IGF-IR-signaling pathway, including IRS-1, the serine/threonine kinase Akt (PKB), and p70 S6 kinase (Fig. 4). The activation of IRS-1 was measured indirectly by an ELISA based on the binding of the p85 subunit of PI3k to the phosphotyrosine residues of
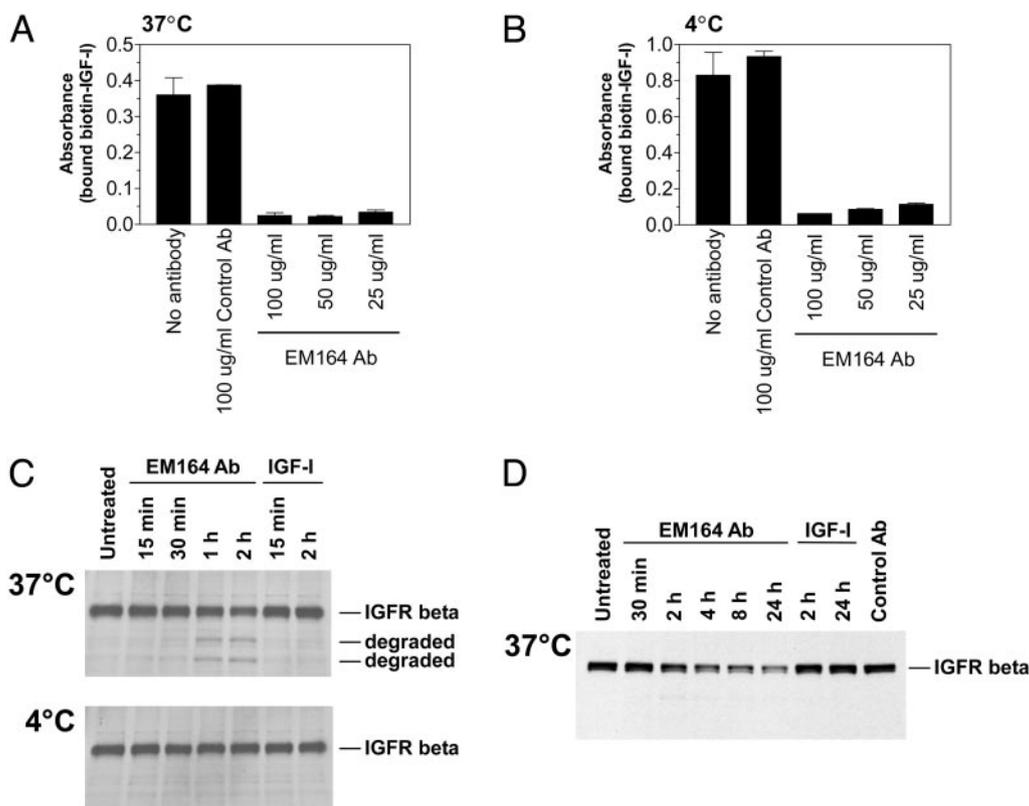
Fig. 3. Inhibition of binding of biotin-IGF-I to IGF-IR on cells by EM164; antibody-mediated down-regulation of IGF-IR. MCF-7 cells were treated with 25–100 μg/ml EM164 for 2 h at 37°C (*A*) or at 4°C (*B*) and then incubated with 50 ng/ml biotinylated IGF-I for 30 min at 37°C (*A*) or 4°C (*B*); cells were washed, lysed, and the lysates were analyzed for biotin-IGF-I bound to IGF-IR using ELISA. *C* and *D*, IGF-IR levels in MCF-7 cells treated with EM164 or IGF-I for 15 min-2 h (or 30 min to 24 h, *D*) at 37°C or at 4°C were analyzed by Western blot using an anti-IGF-IR β chain C-20 antibody.

activated IRS-1 (39). Treatment of MCF-7 cells with EM164 resulted in an almost complete suppression of the IGF-I-stimulated activation of IRS-1 to the basal, unstimulated level (Fig. 4*A*). This inhibition of IRS-1 activation by EM164 was greater than that obtained with the commercially available antibody IR3. Treatment with EM164 alone (in the absence of IGF-I) did not increase IRS-1 activation, thus showing that EM164 has no measurable agonistic activity (Fig. 4*A*).

Similarly, EM164 strongly suppressed the IGF-I-stimulated phosphorylation of Akt and p70/p85 S6 kinase in MCF-7 cells, and again, no agonistic activity could be detected upon treatment with EM164 alone (Fig. 4*B*). Similar results were obtained with the other three cell lines. In addition, EM164 inhibited the IGF-I-stimulated ERK phosphorylation in SaOS-2 cells (data not shown). These results demonstrate that EM164 is a potent inhibitor of the known IGF-IR signal transduction pathway in cancer cell lines *in vitro* and lacks any measurable stimulatory activity.

EM164 Inhibits the Proliferation of Cancer Cells. We then asked the question if this inhibitory activity on the IGF-IR signaling pathway by EM164 was sufficient to affect the proliferation and/or survival of human cancer cell lines *in vitro*. Several cancer cell lines were grown in serum-free medium with exogenously added IGF-I (or IGF-II or serum) in the presence of EM164, typically for ~3 days, and the cell viability was then measured by an MTT assay or by counting live cells. Typically, cells were incubated first with EM164 for about 15 min to 2 h and then treated with IGF-I. In some experiments, cells were incubated first with IGF-I for 15 min before the addition of EM164.

The inhibitory effect of EM164 on the IGF-I-stimulated proliferation, and survival of MCF-7 cells was tested and compared with that of the previously described antibodies IR3 or 1H7 at concentrations

ranging from 0.03 to 20 μg/ml using the MTT assay (Fig. 5*A*). EM164 potently inhibited MCF-7 cell proliferation in a dose-dependent fashion. Significantly, a growth inhibition of ~50% was observed at a 0.2 nM concentration of EM164 (0.03 μg/ml), which was even lower than the concentration of the ligand IGF-I (1.2 nM; 10 ng/ml). EM164 completely inhibited IGF-I-stimulated proliferation at the two highest antibody concentrations tested (4 and 20 μg/ml). Inhibition by EM164 was significantly greater than that of IR3, 1H7 (Fig. 5*A*), and MAB391 (data not shown), showing equivalent inhibition at one-fifth the concentration of these commercially available antibodies (compare 0.03 μg/ml EM164 with 0.16 μg/ml IR3 or 1H7 in Fig. 5*A*). Interestingly, among the antibodies tested, only EM164 was able to suppress the MTT signal below the level observed with the unstimulated control cells (without IGF-I and without antibody), presumably by suppressing the autocrine IGF-IR signaling that promotes proliferation/survival in the absence of exogenously added ligands.

We then tested a large number of human cancer cell lines for their proliferation in response to exogenously added IGF-I and subsequently for their inhibition by EM164. A large majority of cancer cell lines that were tested showed an IGF-I-stimulated proliferation and are listed in Table 1. Treatment with EM164 inhibited the IGF-I-stimulated proliferation and survival in all cell lines tested by 60–100% (Table 1).

The effect of EM164 on serum-stimulated proliferation and survival of MCF-7 cells was then measured by counting of live cells and by MTT assay. MCF-7 cells (initially plated at ~5000 cells/well) were grown in 10% serum in the presence of 5 μg/ml EM164 (or IR3, 1H7, control antibody) for 5 days and then counted. Cultures treated with EM164 had much fewer cells after 5 days than control cultures (16 *versus* 100%), demonstrating that the serum-stimulated prolifer-
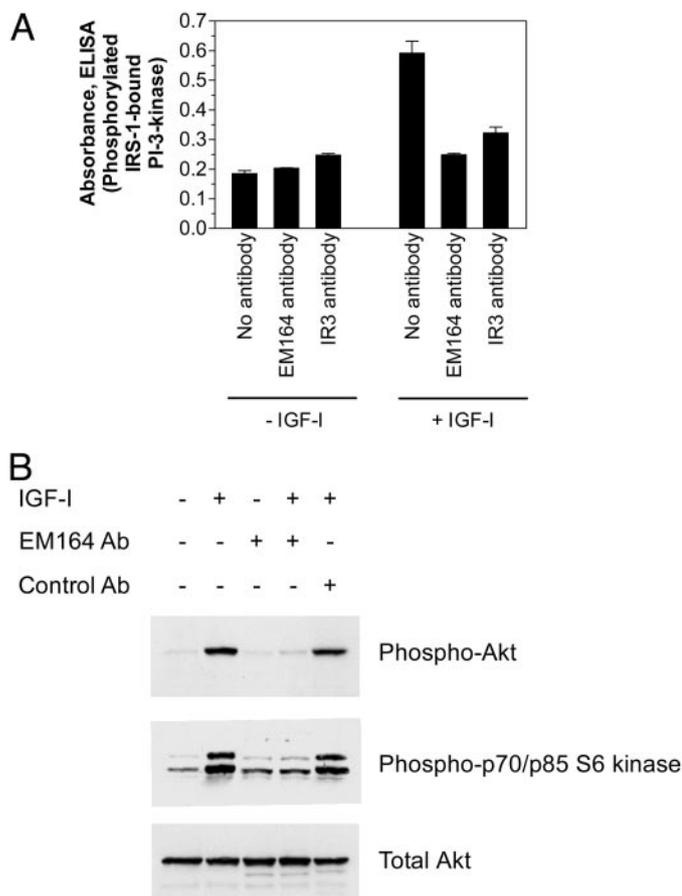
5078

Fig. 4. Inhibition of IGF-I-stimulated signaling in cells by EM164. MCF-7 cells were treated with 10 μg/ml EM164 (or IR3 antibody or a control antibody) for 2 h or overnight at 37°C and then stimulated with IGF-I (50 ng/ml) for 20 min at 37°C. The treated cells were lysed and analyzed for the binding of p85 subunit of PI3k to phosphorylated IRS-1 (*A*) and for the levels of phosphorylation of Akt and p70/p85 S6 kinase (using phospho-specific antibodies) and for total Akt by Western blot (*B*). Similar results were obtained when the cells were incubated with EM164 for 30 min before stimulation with IGF-I for 20 min.

ation of MCF-7 cells was potently inhibited by EM164. In contrast, only a weak inhibition of cell proliferation was seen with IR3 or 1H7 antibody (64 *versus* 100% for control antibody; Fig. 5*B*).

In similar experiments based on the MTT assay after 3 days of growth, EM164 treatment caused 85% inhibition of the serum-stimulated proliferation and survival of MCF-7 and NCI-H838 cells, implicating the essential role of IGF-I as a growth factor present in serum (Fig. 5, *C* and *D*). EM164 inhibited the serum-stimulated proliferation of MCF-7 and NCI-H838 cell lines over many serum concentrations tested (1.25–10% FBS; calf or adult bovine serum) and also in response to IGF-II stimulation (data not shown).

We then explored the question if cells that were first stimulated with IGF-I could still be inhibited in their proliferation and survival by a later incubation with EM164. MCF-7 cells were first activated with IGF-I for 15 min before EM164 was added, and the cell viability was measured after 3 days by MTT assay (Fig. 5*E*). The inhibition by EM164 was similar to that observed when the cells were first incubated with EM164 for 15 min and then IGF-I was added (Fig. 5*E*). In a separate experiment, the simultaneous addition of IGF-I and EM164 also resulted in a potent inhibition, which was similar to that obtained upon an initial incubation with EM164 for 2 h before the addition of IGF-I (data not shown).

EM164 Treatment Causes Cell Cycle Arrest and Apoptosis of Cancer Cells. To further analyze the mechanisms by which EM164 inhibits the proliferation and survival of cancer cells, the effect of

EM164 on the cell cycle of cancer cells was investigated. For cell cycle analysis, MCF-7 cells were treated with IGF-I in the presence or absence of EM164 for 1 day and then analyzed by propidium iodide staining and flow cytometry. The EM164-treated cell population showed a cell cycle distribution very similar to that of unstimulated cells, with most of the cells (77%) in the G_0-G_1 phase, only 9% in the S phase, and 14% in the G_2-M phase. This is in contrast to the IGF-I-stimulated cell population (in the absence of EM164) where 41% of the cells are in the S phase and only 50% in the G_0-G_1 phase (Fig. 6*A*). The cell cycle analysis indicates that EM164 is capable of abrogating most if not all of the mitogenic effect of IGF-I.

To measure the effect of EM164 in a colony formation assay, HT-29 colon cancer cells were plated and grown in serum-containing medium for 10 days in the presence of EM164 or control antibody. Treatment with EM164 resulted in a significant reduction of the colony size compared with that for the control antibody treatment, although the number of colonies was similar (Fig. 6*B*). EM164 treatment, therefore, had a cytostatic effect on the growth of HT-29 colonies in serum.

In addition to its mitogenic role, IGF-IR activation can suppress apoptosis signaling pathways and promote cell survival. To examine the potential effect of EM164 on apoptosis, we used an assay that quantitates the degree of cleavage of the cytokeratin CK18 by activated caspase-3 (60). NCI-H838 lung cancer cells were incubated with IGF-I or serum in the presence or absence of EM164 for 1 day and then assayed for levels of cleaved cytokeratin CK18 protein (Fig. 6*C*). In the absence of EM164, the addition of IGF-I or serum resulted in a lower caspase-cleaved CK18 signal compared with the no IGF-I control, indicating that IGF-I and serum prevent the activation of caspase. Treatment with EM164 suppressed these effects of IGF-I and serum, as indicated by the greater cleaved CK18 levels obtained in the presence of EM164 than in the absence of EM164 (Fig. 6*C*). These results indicate that EM164 can inhibit antiapoptotic signaling by IGF-IR.

***In Vivo* Effect of EM164 on BxPC-3 Human Pancreatic Tumor Xenografts in Mice.** On the basis of the antiproliferative effect of EM164 on cancer cell lines *in vitro*, the antibody was tested *in vivo* for its antitumor effect in a BxPC-3 human pancreatic tumor xenograft model in SCID mice (Fig. 7). Subcutaneous xenografts of BxPC-3 human pancreatic cancer cells were established in SCID/ICR mice until the tumors were ~80 mm³ in size. Groups of animals were then treated by i.v. injections with EM164 alone or in combination with the chemotherapeutic drug gemcitabine as indicated in Fig. 7. The experiment also included three control treatment groups of animals, with one group receiving the vehicle, PBS, the second group gemcitabine alone, and the third group an irrelevant isotype-matched antibody that does not bind to BxPC-3 cells. Treatments started with 12-day-old, established tumors, and the tumor sizes were monitored until day 74, when in all three control groups the tumor size had increased >10-fold to >800 mm³. The tumor growth was similar in all three control groups.

Treatment with EM164 alone or in combination with gemcitabine resulted initially in total regression of tumor xenografts in four of five animals in the EM164 treatment group and in all five animals in the combination treatment group (Fig. 7). Measurable tumor regrowth was only seen in more than one animal on day 43 in the EM164 group and on day 68 in the combination treatment group, resulting in significantly smaller mean tumor volumes on day 74 in comparison with the control treatments ($P = 0.029$ and 0.002, respectively; two-tailed *t* test; $n = 5$/group). Taken together, the pooled EM164 group (including the groups treated with EM164 and with the combination of EM164 and gemcitabine) showed significant reduction in tumor size ($P = 0.0006$; day 74) compared with the pooled control
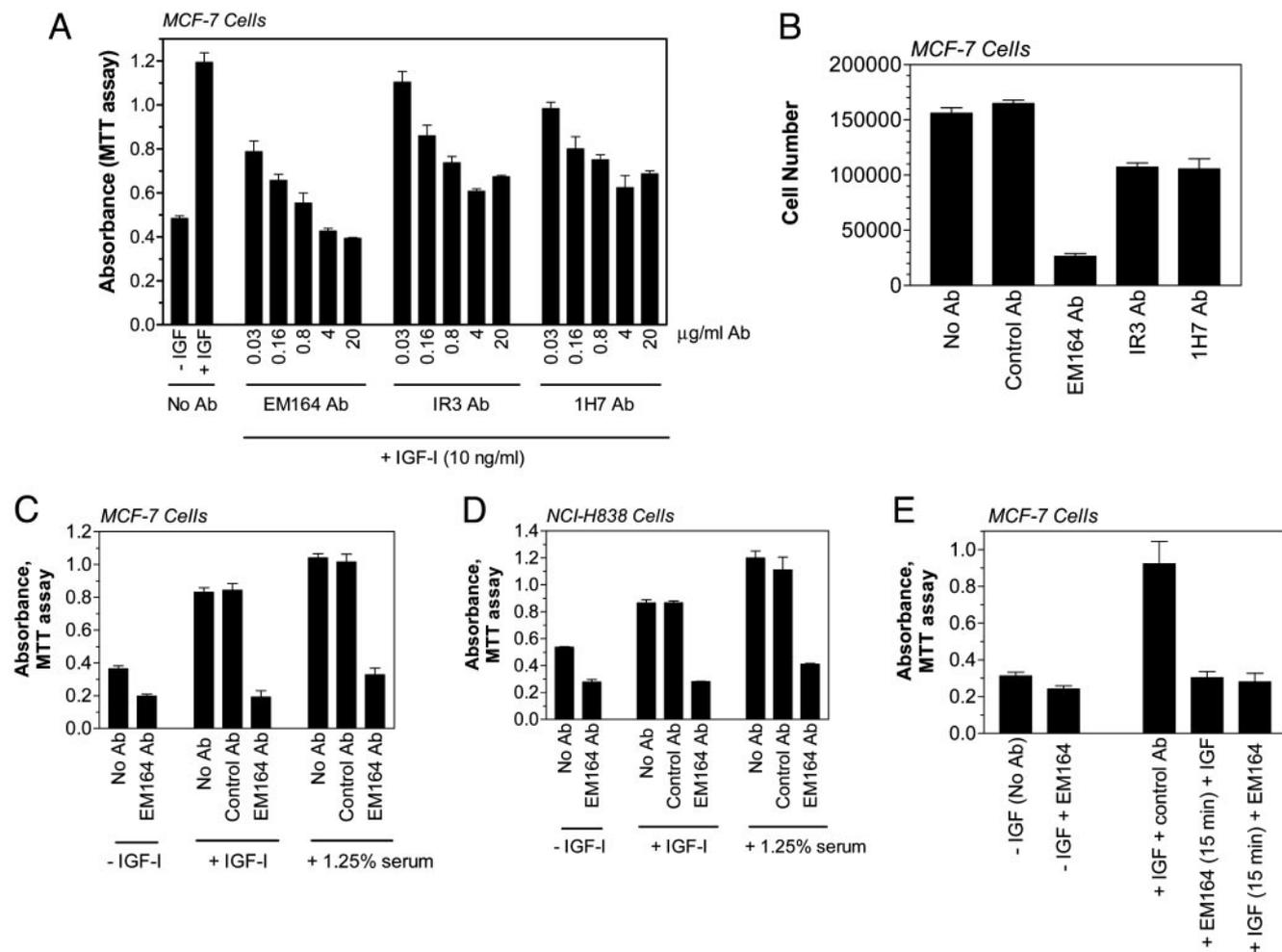
5079

Fig. 5. Potent inhibition of proliferation and survival of cancer cells by EM164. Cancer cells were treated with EM164 in the presence of IGF-I or serum, and the proliferation and survival of cells was monitored using MTT assay (after 3 days) or by cell counting (after 5 days). *A*, comparison of dose-dependent inhibition of IGF-I-stimulated proliferation and survival of MCF-7 cells by EM164 (0.03–20 μg/ml) with that of the commercially available anti-IGF-IR antibodies IR3 and 1H7. *B*, cell counting assay for inhibition of proliferation of MCF-7 cells in 10% serum (5 days) upon treatment with 5 μg/ml EM164, IR3, or 1H7 antibodies. *C* and *D*, inhibition of IGF-I- or serum-stimulated proliferation and survival of breast cancer MCF-7 (*C*) and lung cancer NCI-H838 cells (*D*) by 10 μg/ml EM164. *E*, EM164 was a potent inhibitor of the growth and survival of MCF-7 cells even if added 15 min after the addition of IGF-I, resulting in an inhibition similar to that when EM164 (20 μg/ml) was added 15 min before the addition of IGF-I (10 ng/ml).

group (including the groups treated with PBS, gemcitabine alone, or control antibody). These results indicate that the biological effects observed for EM164 on cancer cell lines *in vitro* may be indicators for *in vivo* antitumor efficacy.

DISCUSSION

A monoclonal antibody EM164 has been developed that binds to the human IGF-I receptor with a high affinity and neutralizes the function of IGF-IR in cancer cells. EM164 inhibits the binding of IGF-I to IGF-IR in cells, blocks the activation of IGF-IR and downstream signaling pathways, and suppresses the biological effects mediated by IGF-IR. Inhibition of IGF-IR function by EM164 resulted in significant anticancer activity both *in vitro*, where EM164 inhibited the growth of diverse cancer cell lines, and *in vivo*, where EM164 treatment suppressed the growth of a pancreatic cancer xenograft.

EM164 proved to be a significantly more potent inhibitor of the IGF-I-stimulated cellular functions of IGF-IR than the commercially available anti-IGF-IR antibodies, IR3, 1H7, and MAB391. The tight binding of EM164 to IGF-IR is likely to be responsible for the potent antagonism of the binding and the activity of the physiological ligand, IGF-I. The K_d of EM164 was measured as 0.1 nM, which is very close to the reported K_d of 0.16 nM for IGF-I (61). Treatment of cells with

EM164 inhibits the binding of IGF-I to IGF-IR at 4°C, a condition wherein no receptor down-regulation is observed. Therefore, the mechanism for the potent inhibition of the binding of IGF-I to IGF-IR by EM164 is likely to be competition for binding, either through sharing of the binding site or through steric exclusion.

In addition to blocking the binding of IGF-I to IGF-IR, EM164 treatment of cells at 37°C causes significant down-regulation of IGF-IR levels, resulting in a 25% decrease in 2 h and a 50–75% decrease in 24 h. The down-regulation of receptor appears to occur by internalization and degradation, as suggested by the detection of degraded IGF-IR β chain in lysates of EM164-treated cells. Similar down-regulation of IGF-IR at 37°C was previously reported (and was confirmed in this study) with the anti-IGF-IR antibodies, IR3, 1H7, and MAB391 (45, 62, 63). This antibody-mediated down-regulation of IGF-IR at 37°C is similar to the antibody-induced degradation of HER-2/ErbB-2 receptor, which is reported to occur through enhanced ubiquitination (64).

Although the inhibitory effect of EM164 on IGF-IR signaling in short-term assays (15 min to 2 h) is most readily explained by the inhibition of the binding of IGF-I to IGF-IR, the antibody-mediated down-regulation of the receptor may also contribute to the inhibitory effects observed in long-term assays such as the IGF-I-stimulated

5080

Table 1 *Inhibition of IGF-I-stimulated proliferation and survival of human cancer cells by EM164 antibody*

Cancer cell type	Fold increase in MTT signal upon IGF-I stimulation[a]	Percentage inhibition of IGF-I-stimulated MTT signal increase by EM164
MCF-7 (breast)	~3	100%
T-47D	1.6	95%
NCI-H838 (lung)	3	100%
Calu-6	1.7	85%
NCI-H1299	1.5	95%
NCI-H460	1.6	80%
NCI-H23	1.6	85%
NCI-H596	1.7	100%
NCI-H441	1.7	60%
HT-3 (cervical)	3	85%
Colo 205 (colon)	2.2	60%
HT-29	1.5	60%
BxPC-3 (pancreatic)	2.1	80%
MiaPaCa-2	2.6	70%
ASPC-1	2.3	75%
A-375 (melanoma)	1.4	70%
M14	1.5	70%
RD (rhabdomyosarcoma)	1.8	95%
SaOS-2 (osteosarcoma)	2.5	100%
Ovcar-5 (ovarian)	1.7	65%
A 431 (epidermoid)	2.2	85%
PC-3 (prostate)	1.3	70%
SK-N-SH (neuroblastoma)	2	85%

[a] MTT assay was performed after 3 days of growth of cancer cells under four conditions: (*a*) no IGF-I, no EM164; (*b*) no IGF-I, + EM164; (*c*) + IGF-I, no EM164; and (*d*) + IGF-I, + EM164. To account for the inhibition of autocrine signaling by EM164, the percentage of inhibition by EM164 was calculated from the MTT assay signals as: $100 \times [((c)-(d))/((c)-(b))]$. Concentrations used were [IGF-I] = 10–20 ng/ml (1.2–2.4 nM) and [EM164 antibody] = 10–20 µg/ml (60–120 nM).

proliferation of cells over a 2–3-day period. The degree of IGF-IR down-regulation by EM164, IR3, 1H7, and MAB391 was similar in these assays. Thus, the superior inhibition observed with EM164 is likely because of the high affinity of EM164 and strong inhibition of IGF-I binding to IGF-IR, rather than an enhanced ability to down-regulate IGF-IR levels.

Treatment with EM164 inhibits the IGF-I-activated signal transduction in cells, resulting in a reduction of the phosphorylation levels of activated IGF-IR and downstream substrates, IRS-1, Akt, and p70 S6 kinase, to levels similar to those present in unstimulated cells. However, it is difficult to predict the biological consequences of inhibitory activity in short-term signal transduction experiments because even a low level of IGF-IR signaling could be above a minimal threshold level required for the proliferation and survival of cells. The effect of the antibody exposure in a long-term assay of proliferation and survival of cancer cells, therefore, may be a better measure of potential *in vivo* biological effects. In this regard, EM164 was significantly more inhibitory than the other three antibodies tested in a 3-day assay of proliferation and survival of MCF-7 breast cancer cells. EM164 inhibited the IGF-I-, IGF-II-, and serum-stimulated proliferation and survival of the large majority of cancer cell lines tested, confirming the important role of IGF-IR in cancer cell growth. Additionally, many cancer cell lines secrete IGF-II and IGF-I for their autocrine growth and survival. We found that EM164 inhibited the autocrine growth of several cancer cell lines (breast cancer MCF-7, T-47D cells, rhabdomyosarcoma RD cells, and lung cancer NCI-

H838, NCI-H596 cells) in serum-free medium lacking exogenously added IGF-I or IGF-II, as indicated by the lower MTT signals obtained upon EM164 treatment than for the untreated cells. The EM164 antibody, therefore, also provides a useful tool for testing the role of autocrine IGF-IR signaling in the growth of cancer cell lines.
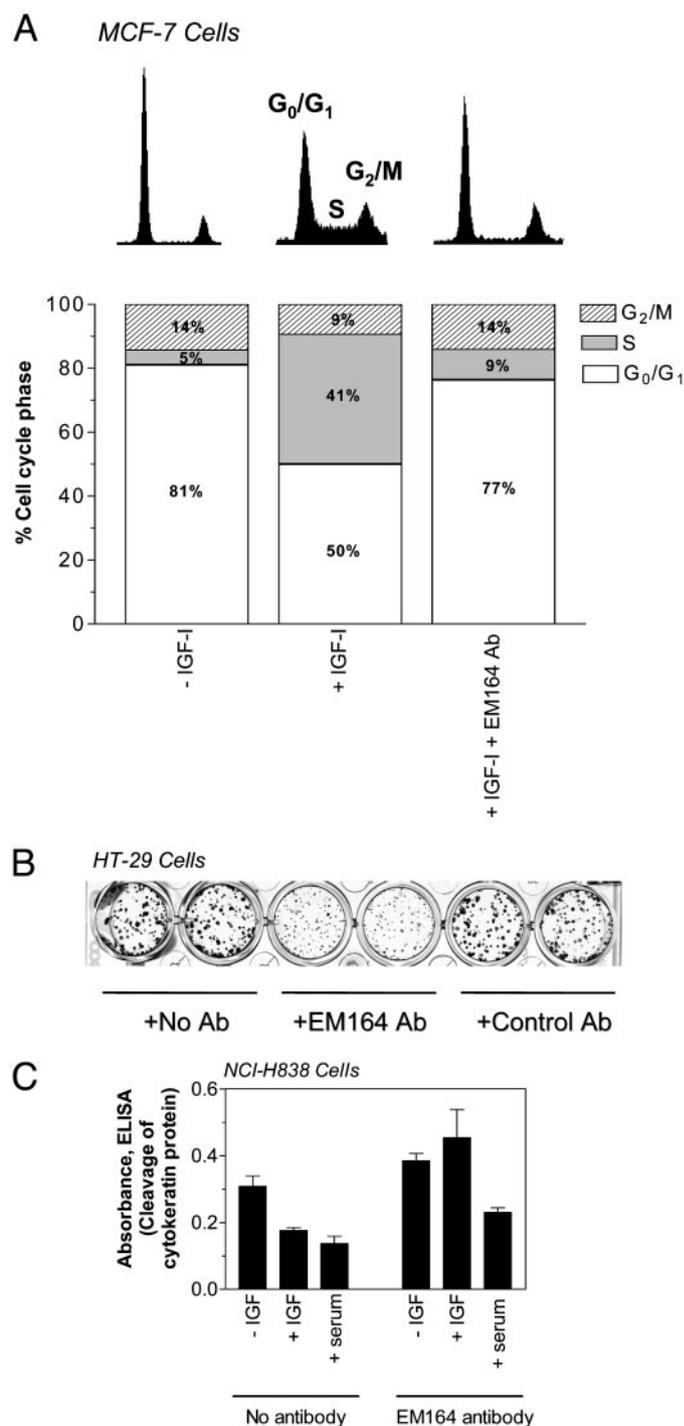

Fig. 6. Cell cycle arrest and induction of apoptosis in cancer cells by treatment with EM164. *A*, MCF-7 cells were treated with EM164 (20 µg/ml) and IGF-I (20 ng/ml) for 1 day and stained with propidium iodide for cell cycle analysis. *B*, growth inhibition of HT-29 colonies by EM164. HT-29 cells (~300 cells initially plated/well) growing in 10% serum were treated with EM164 or control antibody (10 µg/ml) for 10 days and stained with crystal violet. *C*, induction of apoptosis in NCI-H838 cells by EM164; cells were treated with EM164 in the presence or absence of IGF-I or serum for 1 day and analyzed for apoptosis by assay of cleaved cytokeratin CK-18 protein. EM164 suppressed the antiapoptotic effects of IGF-I and serum, as seen by the higher signals in ELISA in the presence of EM164 because of increased apoptosis.
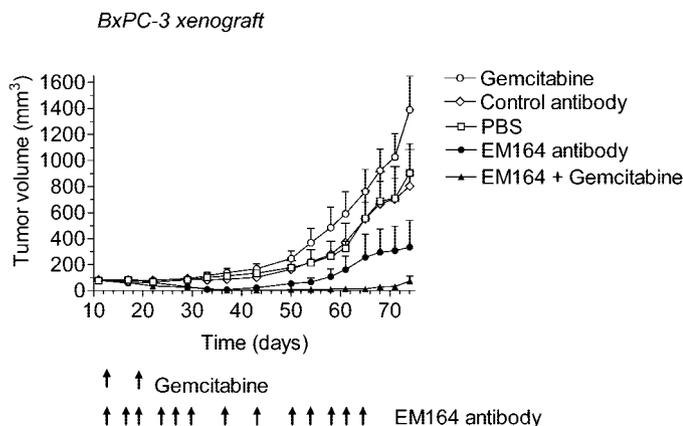
5081

BxPC-3 xenograft

Fig. 7. Suppression of growth of BxPC-3 human pancreatic cancer xenografts in mice by EM164 alone or in combination with gemcitabine. Established BxPC-3 xenografts (80 mm^3) were treated with EM164 (13 injections of 0.8 mg each, i.v.) or gemcitabine (two injections of 150 mg/kg each, i.p.) or a combination of gemcitabine and EM164 antibody or PBS or control antibody or gemcitabine alone. Data plotted are mean ± SE for tumor volume ($n = 5$ each group).

The importance of the IGF-IR in cancer cell growth may be related to both its proliferative and antiapoptotic functions. By blocking receptor activation, EM164 neutralizes all IGF-IR-mediated signal transduction and, in principle, could inhibit cancer cell growth by suppressing cell proliferation or by promoting cell death. The relative contribution of these effects to the anticancer activity of EM164 in different settings (including *in vivo* models) remains to be determined. However, the inhibition of MCF-7 cell growth *in vitro* by EM164 can be attributed principally to a cytostatic effect, where EM164 treatment causes cells to accumulate in the G_0-G_1 state of the cell cycle. EM164 inhibits the proliferation of MCF-7 cells even if it is added 15 min after the activation of cells with the growth factor IGF-I. EM164 is a potent inhibitor of cell proliferation presumably because it suppresses IGF-IR signaling over a sustained period, which is consistent with a study that cell cycle progression into S-phase requires a prolonged activation by the growth factor in two pulses over ~8 h (65).

IGF-I receptor is one of several growth factor receptors (HER2/ErbB2, epidermal growth factor receptor, vascular endothelial growth factor receptor, platelet-derived growth factor receptor, and fibroblast growth factor receptor), which have been implicated in cancer development and progression. These growth factor receptors are under active investigation as targets for cancer therapy using inhibitory antibodies or tyrosine kinase inhibitors (26, 66–68). Because of the distinct biological activities of these receptors, it will be important to compare the effects of their inhibition in clinical settings. Additionally, a combined inhibition of these receptors could prove even more beneficial than targeting each receptor alone. In breast cancer cell models, targeting HER2 and IGF-IR pathways simultaneously is reported to be more effective at inhibiting cell proliferation than targeting a single pathway (69).

The EM164 antibody provides an important reagent for exploring the effect of targeting IGF-IR in xenograft models of several cancers, using the antibody alone or in combination with relevant chemotherapeutic drugs. In this study, treatment of SCID mice bearing established BxPC-3 human pancreatic cancer xenografts with i.v. injections of EM164 led to total tumor regressions, but the tumors eventually regrew. The tumor-free period could be markedly prolonged by combining the antibody treatment with the antipancreatic cancer agent gemcitabine. These findings, together with the broad activity of EM164 on the growth of cancer cells *in vitro*, provide the rationale for additional development of EM164 as a candidate anticancer therapeutic. For potential clinical use, the EM164 antibody has been human-ized to a human IgG with equivalent binding affinity and inhibitory activity.[4]

REFERENCES

1. Khandwala, H. M., McCutcheon, I. E., Flyvbjerg, A., and Friend, K. E. The effects of insulin-like growth factors on tumorigenesis and neoplastic growth. Endocr. Rev., *21:* 215–244, 2000.
2. Baserga, R., Hongo, A., Rubini, M., Prisco, M., and Valentinis, B. The IGF-I receptor in cell growth, transformation and apoptosis. Biochim. Biophys. Acta, *1332:* F105–F126, 1997.
3. Blakesley, V. A., Stannard, B. S., Kalebic, T., Helman, L. J., and LeRoith, D. Role of the IGF-I receptor in mutagenesis and tumor promotion. J. Endocrinol., *152:* 339–344, 1997.
4. Kaleko, M., Rutter, W. J., and Miller, A. D. Overexpression of the human insulin-like growth factor I receptor promotes ligand-dependent neoplastic transformation. Mol. Cell. Biol., *10:* 464–473, 1990.
5. Weber, M. M., Fottner, C., Liu, S. B., Jung, M. C., Engelhardt, D., and Baretton, G. B. Overexpression of the insulin-like growth factor I receptor in human colon carcinomas. Cancer (Phila.), *95:* 2086–2095, 2002.
6. Hellawell, G. O., Turner, G. D., Davies, D. R., Poulsom, R., Brewster, S. F., and Macaulay, V. M. Expression of the type 1 insulin-like growth factor receptor is up-regulated in primary prostate cancer and commonly persists in metastatic disease. Cancer Res., *62:* 2942–2950, 2002.
7. Werner, H., and LeRoith, D. The role of the insulin-like growth factor system in human cancer. Adv. Cancer Res., *68:* 183–223, 1996.
8. Happerfield, L. C., Miles, D. W., Barnes, D. M., Thomsen, L. L., Smith, P., and Hanby, A. The localization of the insulin-like growth factor receptor I (IGFR-I) in benign and malignant breast tissue. J. Pathol., *183:* 412–417, 1997.
9. Xie, Y., Skytting, B., Nilsson, G., Brodin, B., and Larsson, O. Expression of insulin-like growth factor I receptor in synovial sarcoma: association with an aggressive phenotype. Cancer Res., *59:* 3588–3591, 1999.
10. Bergmann, U., Funatomi, H., Yokoyama, M., Beger, H. G., and Korc, M. Insulin-like growth factor I overexpression in human pancreatic cancer: evidence for autocrine and paracrine roles. Cancer Res., *55:* 2007–2011, 1995.
11. Cullen, K. J., Yee, D., Sly, W. S., Perdue, J., Hampton, B., Lippman, M. E., and Rosen, N. Insulin-like growth factor receptor expression and function in human breast cancer. Cancer Res., *50:* 48–53, 1990.
12. Hermanto, U., Zong, C. S., and Wang, L. H. Inhibition of mitogen-activated protein kinase kinase selectively inhibits cell proliferation in human breast cancer cells displaying enhanced insulin-like growth factor I-mediated mitogen-activated protein kinase activation. Cell Growth Differ., *11:* 655–664, 2000.
13. Ankrapp, D. P., and Bevan, D. R. Insulin-like growth factor-I and human lung fibroblast-derived insulin-like growth factor I stimulate the proliferation of human lung carcinoma cells *in vitro*. Cancer Res., *53:* 3399–3404, 1993.
14. Guo, Y. S., Jin, G. F., Townsend, C. M., Jr., Zhang, T., Sheng, H. M., Beauchamp, R. D., and Thompson, J. C. Insulin-like growth factor II expression in carcinoma in colon cell lines: implications for autocrine actions. J. Am. Coll. Surg., *181:* 145–154, 1995.
15. Kappel, C. C., Velez-Yanguas, M. C., Hirschfeld, S., and Helman, L. J. Human osteosarcoma cell lines are dependent on insulin-like growth factor I for *in vitro* growth. Cancer Res., *54:* 2803–2807, 1994.
16. Steller, M. A., Delgado, C. H., Bartels, C. J., Woodworth, C. D., and Zou, Z. Overexpression of the insulin-like growth factor I receptor and autocrine stimulation in human cervical cancer cells. Cancer Res., *56:* 1761–1765, 1996.
17. Quinn, K. A., Treston, A. M., Unsworth, E. J., Miller, M. J., Vos, M., Grimley, C., Battey, J., Mulshine, J. L., and Cuttitta, F. Insulin-like growth factor expression in human cancer cell lines. J. Biol. Chem., *271:* 11477–11483, 1996.
18. Chan, J. M., Stampfer, M. J., Giovannucci, E., Gann, P. H., Ma, J., Wilkinson, P., Hennekens, C. H., and Pollak, M. Plasma insulin-like growth factor I and prostate cancer risk: a prospective study. Science (Wash. DC), *279:* 563–566, 1998.
19. Wolk, A., Mantzoros, C. S., Andersson, S. O., Bergstrom, R., Signorello, L. B., Lagiou, P., Adami, H. O., and Trichopoulos, D. Insulin-like growth factor I and prostate cancer risk: a population-based, case-control study. J. Natl. Cancer Inst. (Bethesda), *90:* 911–915, 1998.
20. Ma, J., Pollak, M. N., Giovannucci, E., Chan, J. M., Tao, Y., Hennekens, C. H., and Stampfer, M. J. Prospective study of colorectal cancer risk in men and plasma levels of insulin-like growth factor (IGF)-I and IGF-binding protein-3. J. Natl. Cancer Inst. (Bethesda), *91:* 620–625, 1999.
21. Yu, H., Spitz, M. R., Mistry, J., Gu, J., Hong, W. K., and Wu, X. Plasma levels of insulin-like growth factor I and lung cancer risk: a case-control analysis. J. Natl. Cancer Inst. (Bethesda), *91:* 151–156, 1999.
22. Hankinson, S. E., Willett, W. C., Colditz, G. A., Hunter, D. J., Michaud, D. S., Deroo, B., Rosner, B., Speizer, F. E., and Pollak, M. Circulating concentrations of insulin-like growth factor I and risk of breast cancer. Lancet, *351:* 1393–1396, 1998.

---

[4] D. Tavares and R. Singh, unpublished results.

23. Navarro, M., and Baserga, R. Limited redundancy of survival signals from the type 1 insulin-like growth factor receptor. Endocrinology, *142:* 1073–1081, 2001.

24. Harrington, E. A., Bennett, M. R., Fanidi, A., and Evan, G. I. c-Myc-induced apoptosis in fibroblasts is inhibited by specific cytokines. EMBO J., *13:* 3286–3295, 1994.

25. Adachi, Y., Lee, C. T., Coffee, K., Yamagata, N., Ohm, J. E., Park, K. H., Dikov, M. M., Nadaf, S. R., Arteaga, C. L., and Carbone, D. P. Effects of genetic blockade of the insulin-like growth factor receptor in human colon cancer cell lines. Gastroenterology, *123:* 1191–1204, 2002.

26. Reinmuth, N., Liu, W., Fan, F., Jung, Y. D., Ahmad, S. A., Stoeltzing, O., Bucana, C. D., Radinsky, R., and Ellis, L. M. Blockade of insulin-like growth factor I receptor function inhibits growth and angiogenesis of colon cancer. Clin. Cancer Res., *8:* 3259–3269, 2002.

27. Resnicoff, M., Coppola, D., Sell, C., Rubin, R., Ferrone, S., and Baserga, R. Growth inhibition of human melanoma cells in nude mice by antisense strategies to the type 1 insulin-like growth factor receptor. Cancer Res., *54:* 4848–4850, 1994.

28. Lee, C. T., Wu, S., Gabrilovich, D., Chen, H., Nadaf-Rahrov, S., Ciernik, I. F., and Carbone, D. P. Antitumor effects of an adenovirus expressing antisense insulin-like growth factor I receptor on human lung cancer cell lines. Cancer Res., *56:* 3038–3041, 1996.

29. Muller, M., Dietel, M., Turzynski, A., and Wiechen, K. Antisense phosphorothioate oligodeoxynucleotide down-regulation of the insulin-like growth factor I receptor in ovarian cancer cells. Int. J. Cancer, *77:* 567–571, 1998.

30. Seely, B. L., Samimi, G., and Webster, N. J. Retroviral expression of a kinase-defective IGF-I receptor suppresses growth and causes apoptosis of CHO and U87 cells *in vivo*. BMC Cancer, *2:* 15, 2002.

31. Liu, X., Turbyville, T., Fritz, A., and Whitesell, L. Inhibition of insulin-like growth factor I receptor expression in neuroblastoma cells induces the regression of established tumors in mice. Cancer Res., *58:* 5432–5438, 1998.

32. Shapiro, D. N., Jones, B. G., Shapiro, L. H., Dias, P., and Houghton, P. J. Antisense-mediated reduction in insulin-like growth factor-I receptor expression suppresses the malignant phenotype of a human alveolar rhabdomyosarcoma. J. Clin. Investig., *94:* 1235–1242, 1994.

33. Resnicoff, M., Abraham, D., Yutanawiboonchai, W., Rotman, H. L., Kajstura, J., Rubin, R., Zoltick, P., and Baserga, R. The insulin-like growth factor I receptor protects tumor cells from apoptosis *in vivo*. Cancer Res., *55:* 2463–2469, 1995.

34. Baserga, R. The insulin-like growth factor I receptor: a key to tumor growth? Cancer Res., *55:* 249–252, 1995.

35. LeRoith, D., Werner, H., Beitner-Johnson, D., and Roberts, C. T., Jr. Molecular and cellular aspects of the insulin-like growth factor I receptor. Endocr. Rev., *16:* 143–163, 1995.

36. Dufourny, B., Alblas, J., van Teeffelen, H. A., van Schaik, F. M., van der Burg, B., Steenbergh, P. H., and Sussenbach, J. S. Mitogenic signaling of insulin-like growth factor I in MCF-7 human breast cancer cells requires phosphatidylinositol 3-kinase and is independent of mitogen-activated protein kinase. J. Biol. Chem., *272:* 31163–31171, 1997.

37. Parrizas, M., Gazit, A., Levitzki, A., Wertheimer, E., and LeRoith, D. Specific inhibition of insulin-like growth factor I and insulin receptor tyrosine kinase activity and biological function by tyrphostins. Endocrinology, *138:* 1427–1433, 1997.

38. Kulik, G., Klippel, A., and Weber, M. J. Antiapoptotic signalling by the insulin-like growth factor I receptor, phosphatidylinositol 3-kinase, and Akt. Mol. Cell. Biol., *17:* 1595–1606, 1997.

39. Jackson, J. G., White, M. F., and Yee, D. Insulin receptor substrate-1 is the predominant signaling molecule activated by insulin-like growth factor-I, insulin, and interleukin-4 in estrogen receptor-positive human breast cancer cells. J. Biol. Chem., *273:* 9994–10003, 1998.

40. Datta, S. R., Brunet, A., and Greenberg, M. E. Cellular survival: a play in three Akts. Genes Dev., *13:* 2905–2927, 1999.

41. Ullrich, A., Gray, A., Tam, A. W., Yang-Feng, T., Tsubokawa, M., Collins, C., Henzel, W., Le Bon, T., Kathuria, S., Chen, E., Jacobs, S., Francke, U., Ramachandran, J., and Fujita-Yamaguchi, Y. Insulin-like growth factor I receptor primary structure: comparison with insulin receptor suggests structural determinants that define functional specificity. EMBO J., *5:* 2503–2512, 1986.

42. Fujita-Yamaguchi, Y., LeBon, T. R., Tsubokawa, M., Henzel, W., Kathuria, S., Koyal, D., and Ramachandran, J. Comparison of insulin-like growth factor I receptor and insulin receptor purified from human placental membranes. J. Biol. Chem., *261:* 16727–16731, 1986.

43. Rohlik, Q. T., Adams, D., Kull, F. C., Jr., and Jacobs, S. An antibody to the receptor for insulin-like growth factor I inhibits the growth of MCF-7 cells in tissue culture. Biochem. Biophys. Res. Commun., *149:* 276–281, 1987.

44. Kalebic, T., Tsokos, M., and Helman, L. J. *In vivo* treatment with antibody against IGF-I receptor suppresses growth of human rhabdomyosarcoma and down-regulates p34cdc2. Cancer Res., *54:* 5531–5534, 1994.

45. Zia, F., Jacobs, S., Kull, F., Jr., Cuttitta, F., Mulshine, J. L., and Moody, T. W. Monoclonal antibody α IR-3 inhibits non-small cell lung cancer growth *in vitro* and *in vivo*. J. Cell. Biochem. Suppl., *24:* 269–275, 1996.

46. Scotlandi, K., Benini, S., Nanni, P., Lollini, P. L., Nicoletti, G., Landuzzi, L., Serra, M., Manara, M. C., Picci, P., and Baldini, N. Blockage of insulin-like growth factor I receptor inhibits the growth of Ewing's sarcoma in athymic mice. Cancer Res., *58:* 4127–4131, 1998.

47. Kato, H., Faria, T. N., Stannard, B., Roberts, C. T., Jr., and LeRoith, D. Role of tyrosine kinase activity in signal transduction by the insulin-like growth factor I (IGF-I) receptor. Characterization of kinase-deficient IGF-I receptors and the action of an IGF-I-mimetic antibody (α IR-3). J. Biol. Chem., *268:* 2655–2661, 1993.

48. Steele-Perkins, G., and Roth, R. A. Monoclonal antibody alpha IR-3 inhibits the ability of insulin-like growth factor II to stimulate a signal from the type I receptor without inhibiting its binding. Biochem. Biophys. Res. Commun., *171:* 1244–1251, 1990.

49. Arteaga, C. L., Kitten, L. J., Coronado, E. B., Jacobs, S., Kull, F. C., Jr., Allred, D. C., and Osborne, C. K. Blockade of the type I somatomedin receptor inhibits growth of human breast cancer cells in athymic mice. J. Clin. Investig., *84:* 1418–1423, 1989.

50. Soos, M. A., Field, C. E., Lammers, R., Ullrich, A., Zhang, B., Roth, R. A., Andersen, A. S., Kjeldsen, T., and Siddle, K. A panel of monoclonal antibodies for the type I insulin-like growth factor receptor. Epitope mapping, effects on ligand binding, and biological activity. J. Biol. Chem., *267:* 12955–12963, 1992.

51. Li, S. L., Kato, J., Paz, I. B., Kasuya, J., and Fujita-Yamaguchi, Y. Two new monoclonal antibodies against the α subunit of the human insulin-like growth factor I receptor. Biochem. Biophys. Res. Commun., *196:* 92–98, 1993.

52. Miura, M., Surmacz, E., Burgaud, J. L., and Baserga, R. Different effects on mitogenesis and transformation of a mutation at tyrosine 1251 of the insulin-like growth factor I receptor. J. Biol. Chem., *270:* 22639–22644, 1995.

53. Singh, R., and Maloney, E. K. Labeling of antibodies by *in situ* modification of thiol groups generated from selenol-catalyzed reduction of native disulfide bonds. Anal. Biochem., *304:* 147–156, 2002.

54. Langone, J., and Vunakis, H. Immunochemical Techniques, Part I, Vol. 121. Orlando: Academic, 1986.

55. Harlow, E., and Lane, D., Antibodies: A Laboratory Manual. Cold Spring Harbor: Cold Spring Harbor Laboratory, 1988.

56. Singh, R., and Whitesides, G. M. Thiol-disulfide interchange. *In:* S. Patai, and Z. Rappoport, Z. (eds.), Supplement S: The Chemistry of Sulphur-containing Functional Groups, pp. 633–658. Chichester: Wiley, 1993.

57. Kristensen, C., Wiberg, F. C., and Andersen, A. S. Specificity of insulin and insulin-like growth factor I receptors investigated using chimeric mini-receptors. Role of C-terminal of receptor α subunit. J. Biol. Chem., *274:* 37351–37356, 1999.

58. Molina, L., Marino-Buslje, C., Quinn, D. R., and Siddle, K. Structural domains of the insulin receptor and IGF receptor required for dimerisation and ligand binding. FEBS Lett., *467:* 226–230, 2000.

59. Rice, G. E., Munro, J. M., Corless, C., and Bevilacqua, M. P. Vascular and nonvascular expression of INCAM-110. A target for mononuclear leukocyte adhesion in normal and inflamed human tissues. Am. J. Pathol., *138:* 385–393, 1991.

60. MacFarlane, M., Merrison, W., Dinsdale, D., and Cohen, G. M. Active caspases and cleaved cytokeratins are sequestered into cytoplasmic inclusions in TRAIL-induced apoptosis. J. Cell Biol., *148:* 1239–1254, 2000.

61. Schumacher, R., Soos, M. A., Schlessinger, J., Brandenburg, D., Siddle, K., and Ullrich, A. Signaling-competent receptor chimeras allow mapping of major insulin receptor binding domain determinants. J. Biol. Chem., *268:* 1087–1094, 1993.

62. Hailey, J., Maxwell, E., Koukouras, K., Bishop, W. R., Pachter, J. A., and Wang, Y. Neutralizing anti-insulin-like growth factor receptor 1 antibodies inhibit receptor function and induce receptor degradation in tumor cells. Mol. Cancer Ther., *1:* 1349–1353, 2002.

63. Sachdev, D., Li, S. L., Hartell, J. S., Fujita-Yamaguchi, Y., Miller, J. S., and Yee, D. A Chimeric humanized single-chain antibody against the type I insulin-like growth factor (IGF) receptor renders breast cancer cells refractory to the mitogenic effects of IGF-I. Cancer Res., *63:* 627–635, 2003.

64. Klapper, L. N., Waterman, H., Sela, M., and Yarden, Y. Tumor inhibitory antibodies to HER-2/ErbB-2 may act by recruiting c-Cbl and enhancing ubiquitination of HER-2. Cancer Res., *60:* 3384–3388, 2000.

65. Jones, S. M., and Kazlauskas, A. Growth factor-dependent signaling and cell cycle progression. FEBS Lett., *490:* 110–116, 2001.

66. Baselga, J. Why the epidermal growth factor receptor? The rationale for cancer therapy. Oncologist, *7* (Suppl. 4)*:* 2–8, 2002.

67. Pegram, M., Hsu, S., Lewis, G., Pietras, R., Beryt, M., Sliwkowski, M., Coombs, D., Baly, D., Kabbinavar, F., and Slamon, D. Inhibitory effects of combinations of HER-2/neu antibody and chemotherapeutic agents used for treatment of human breast cancers. Oncogene, *18:* 2241–2251, 1999.

68. Lopez, T., and Hanahan, D. Elevated levels of IGF-1 receptor convey invasive and metastatic capability in a mouse model of pancreatic islet tumorigenesis. Cancer Cell, *1:* 339–353, 2002.

69. Lu, Y., Zi, X., Zhao, Y., Mascarenhas, D., and Pollak, M. Insulin-like growth factor I receptor signaling and resistance to trastuzumab (Herceptin). J. Natl. Cancer Inst. (Bethesda), *93:* 1852–1857, 2001.

An Anti-Insulin-like Growth Factor I Receptor Antibody That Is a Potent Inhibitor of Cancer Cell Proliferation

Erin K. Maloney, Jennifer L. McLaughlin, Nancy E. Dagdigian, et al.

Updated version	Access the most recent version of this article at: http://cancerres.aacrjournals.org/content/63/16/5073

Cited articles	This article cites 64 articles, 35 of which you can access for free at: http://cancerres.aacrjournals.org/content/63/16/5073.full#ref-list-1
Citing articles	This article has been cited by 65 HighWire-hosted articles. Access the articles at: http://cancerres.aacrjournals.org/content/63/16/5073.full#related-urls

E-mail alerts	Sign up to receive free email-alerts related to this article or journal.
Reprints and Subscriptions	To order reprints of this article or to subscribe to the journal, contact the AACR Publications Department at pubs@aacr.org.
Permissions	To request permission to re-use all or part of this article, use this link http://cancerres.aacrjournals.org/content/63/16/5073. Click on "Request Permissions" which will take you to the Copyright Clearance Center's (CCC) Rightslink site.